Supporting Information

Luo et al. 10.1073/pnas.1210239109

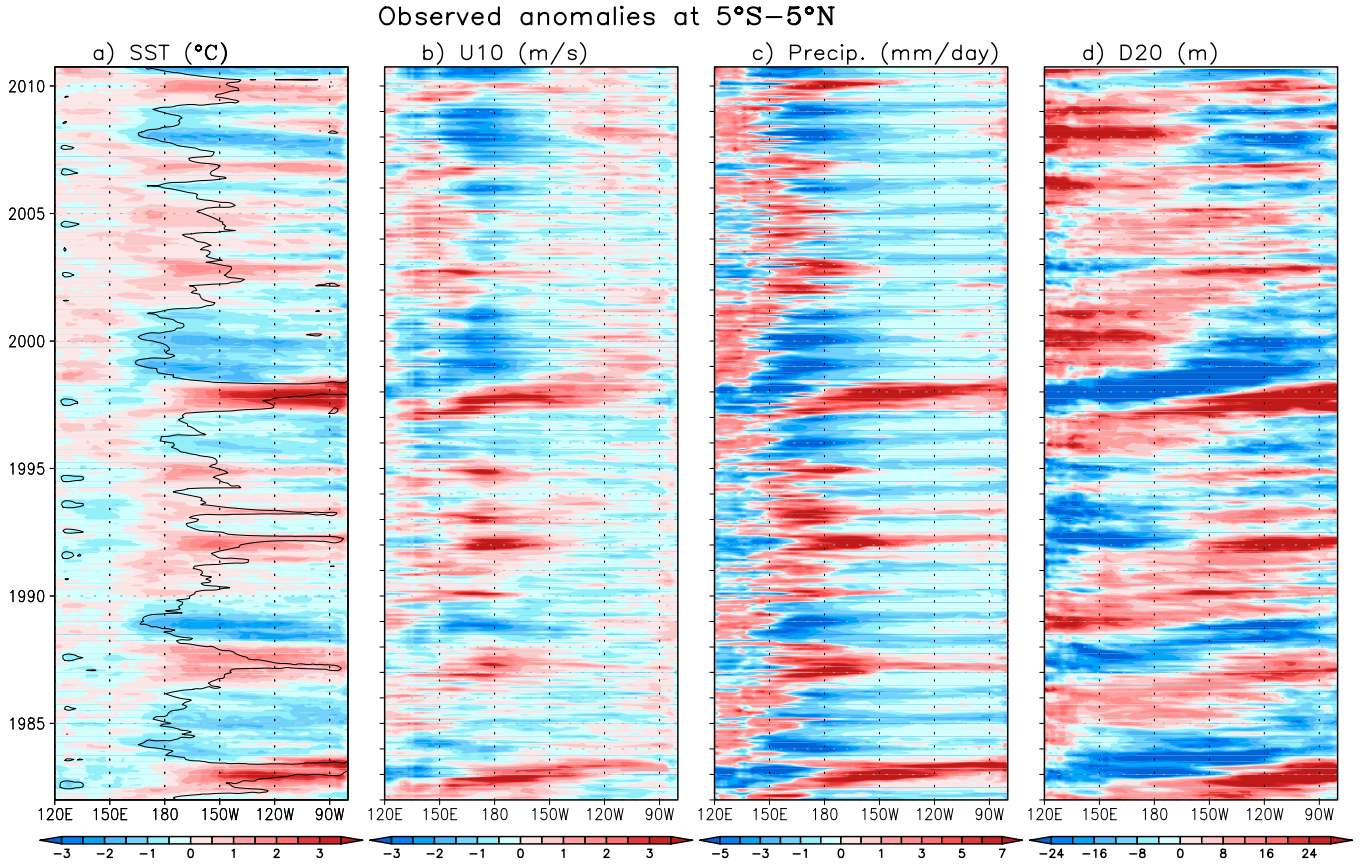

Fig. S1. Changing El Niño behaviors in the 2000s. Shown are observed sea surface temperature (SST), zonal surface wind, precipitation, and ocean 20 °C isotherm depth anomalies (relative to the climatology of 1983–2006) in the equatorial Pacific (5°S–5°N) during 1982–2010. The solid line in *A* denotes the 28 °C isotherm of SST.

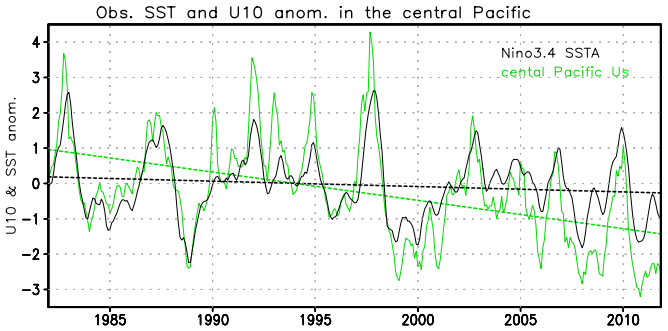

Fig. S2. SST and trade winds in the central Pacific. Shown are observed SST anomalies (solid black line) at Niño3.4 area (190°–240°E, 5°S–5°N) and surface zonal wind anomalies (solid green line) in the central Pacific (160°–190°E, 5°S–5°N). Dashed lines display their linear trends. Compared with the previous decades, the central-Pacific easterlies persistently increased in both El Niño and La Niña years during the last decade.

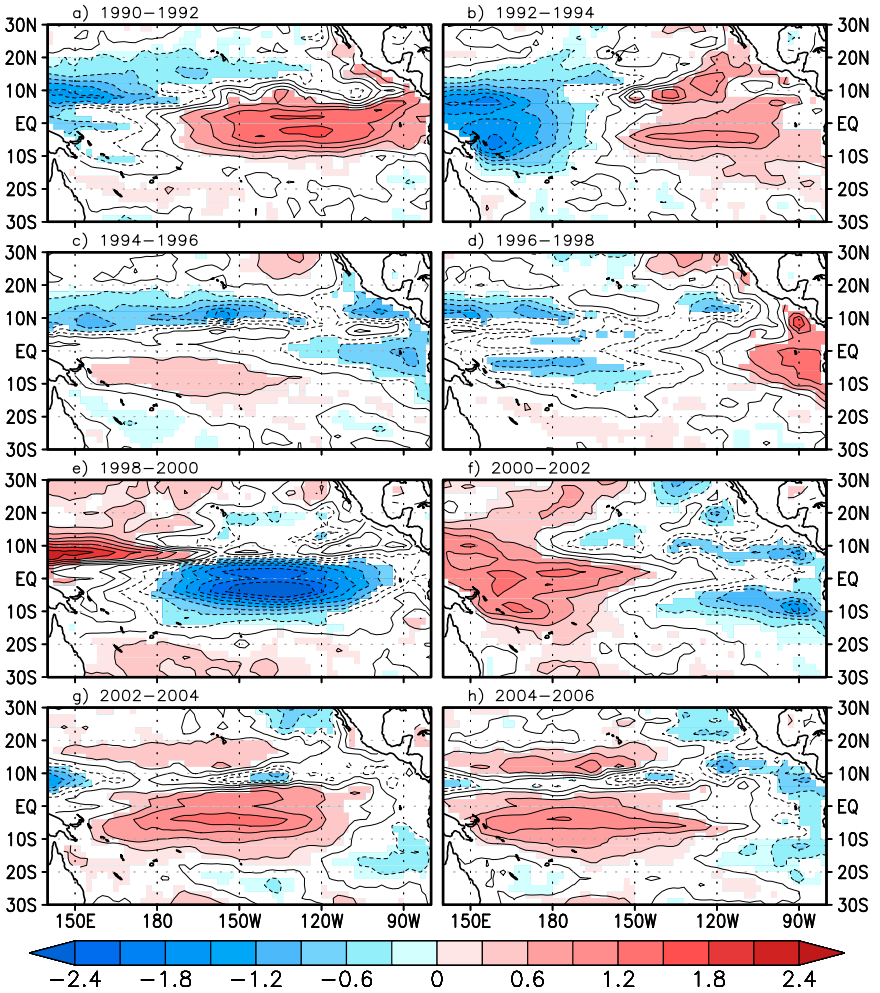

Fig. S3. Ocean subsurface temperature anomalies in the Pacific. Shown are 3-y mean ocean temperature anomalies (color shadings indicate ≤5% significance according to one-tailed Student *t* test) averaged at the potential density layers between $\sigma\theta = 23.1$ and $\sigma\theta = 26.1$, which represents the lower and upper layer of the equatorial Pacific thermocline. These are ensemble means of seven ocean reanalysis data sets [NCEP GODAS, United Kingdom Met Office DePreSys, The European Centre for Medium-Range Weather Forecasts (ECMWF) NEMOVAR COMBINE, ECMWF Ocean Reanalysis System 3, ECMWF Ocean Reanalysis-XBTc, Simple Ocean Data Assimilation (SODA)2.1.6, and SODA2.2.4. Detailed information is available on http://icdc.zmaw.de/easy_init_ocean.html?&L=1]. We could not find reliable evidence among different ocean reanalysis data to confirm the hypothesis that subsurface signals originating from the extratropical oceans are responsible for the La Niña-like state in the 2000s. The decadal mean equatorial Pacific warm water volume during the 2000s is actually above normal (see also www.pmel.noaa.gov/tao/elnino/wwv/).

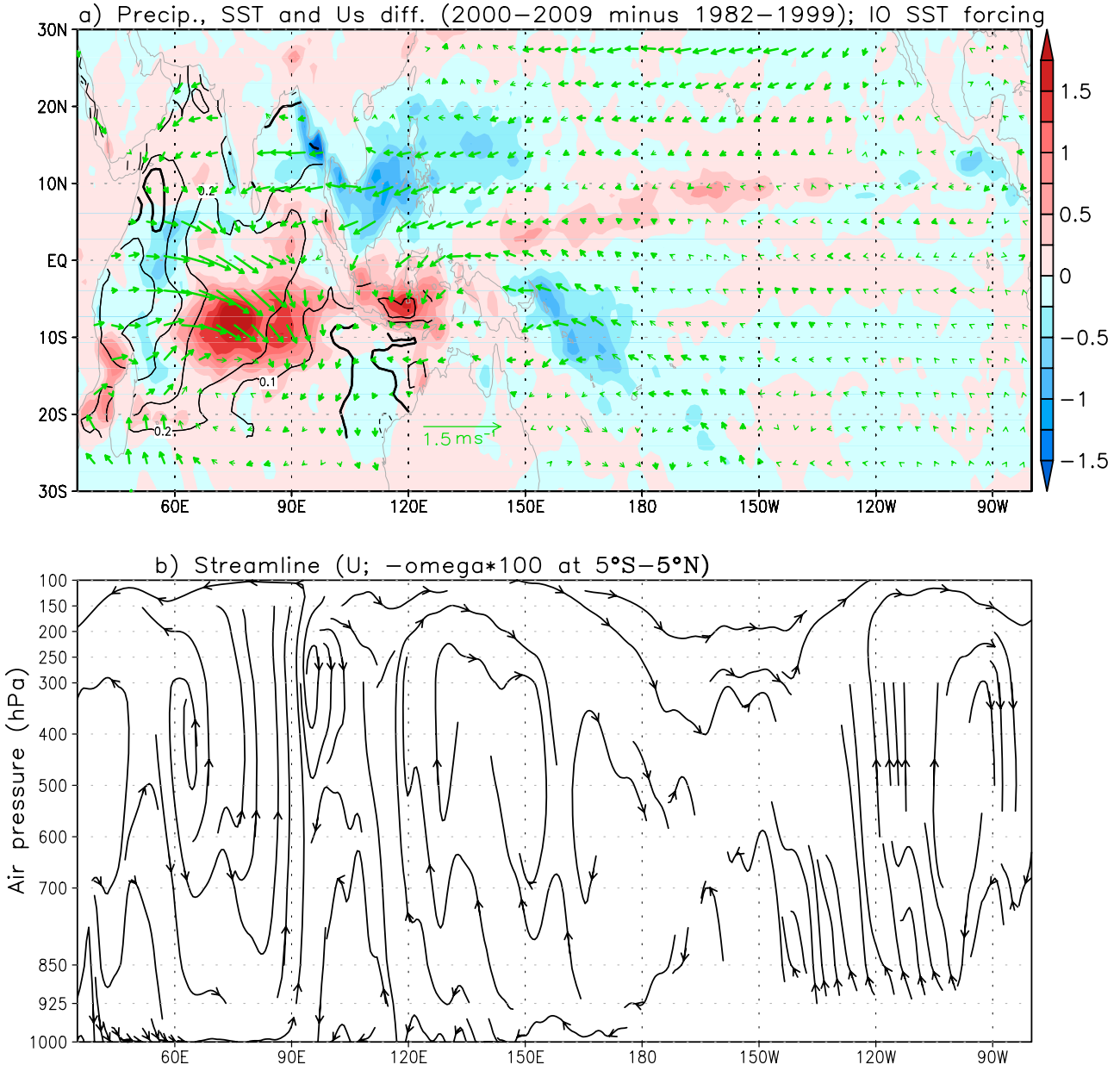

Fig. S4. Influence of the recent Indian Ocean (IO) warming trend on the Pacific atmosphere. Shown are (*A*) surface winds (thick vectors indicate ≤5% significance according to two-tailed Student *t* test) and precipitation (mm/d, color scaled) changes caused by the IO SST rise (2000–2009 minus 1982–1999, contour). (*B*) As in *A*, but for the east–west Walker circulation change in the equatorial zone. These are based on nine-member ensemble mean of model experiments in which observed SSTs only the tropical IO are assimilated into the coupled model, whereas climatological SSTs are prescribed elsewhere.

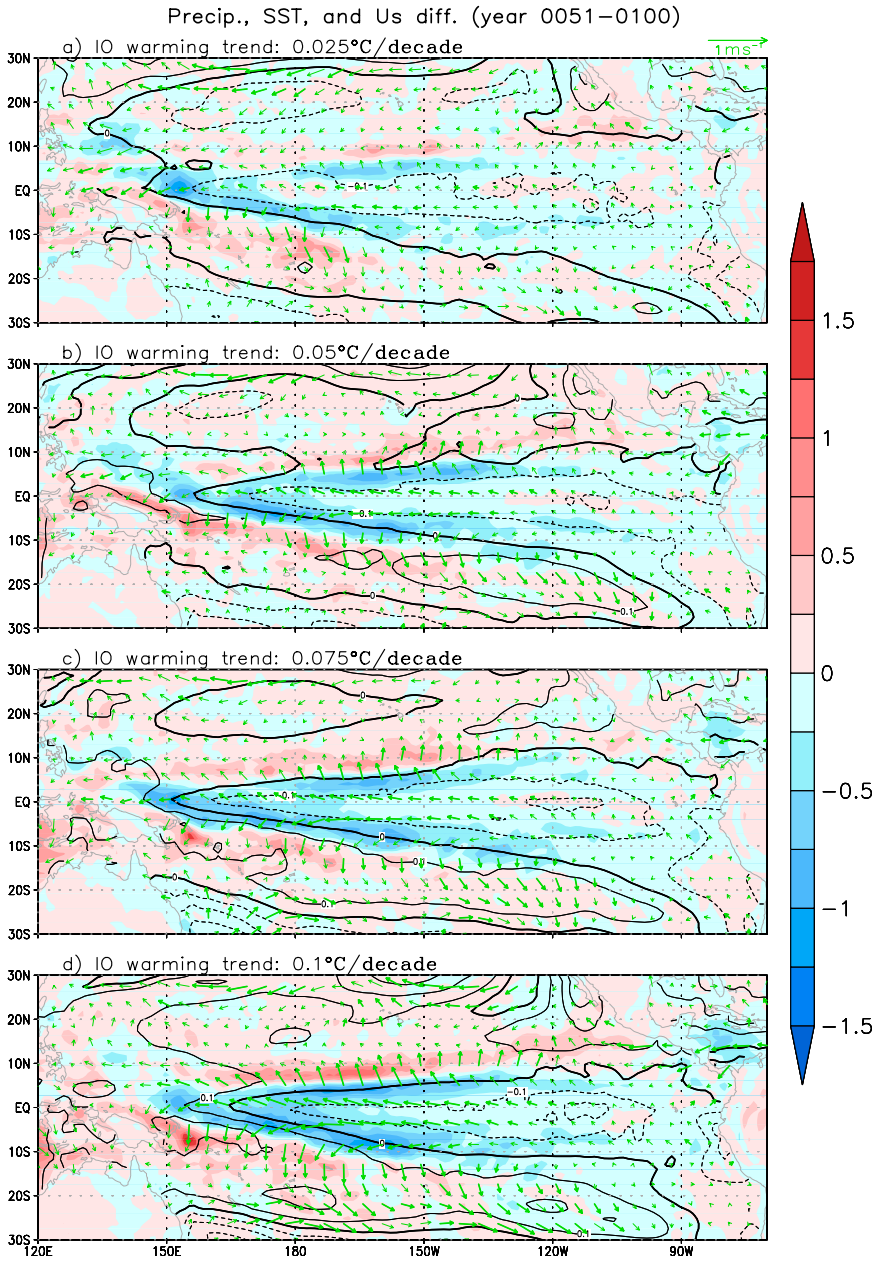

Fig. S5. Influence of multidecadal IO warming on the Pacific, according to climate model experiments. Shown are 50-y mean differences of SST (contour), surface winds (thick vectors denote ≤10% significance according to two-tailed Student *t* test), and precipitation (mm/d, color scaled) between the model sensitivity experiments and control run. In the control run, model climatological SST is prescribed in the tropical IO but with free ocean–atmosphere coupling elsewhere. In the sensitivity experiments, four linear warming trends (0.025, 0.05, 0.075, and 0.1 °C per decade, relative to the Pacific's) are added in the tropical IO.

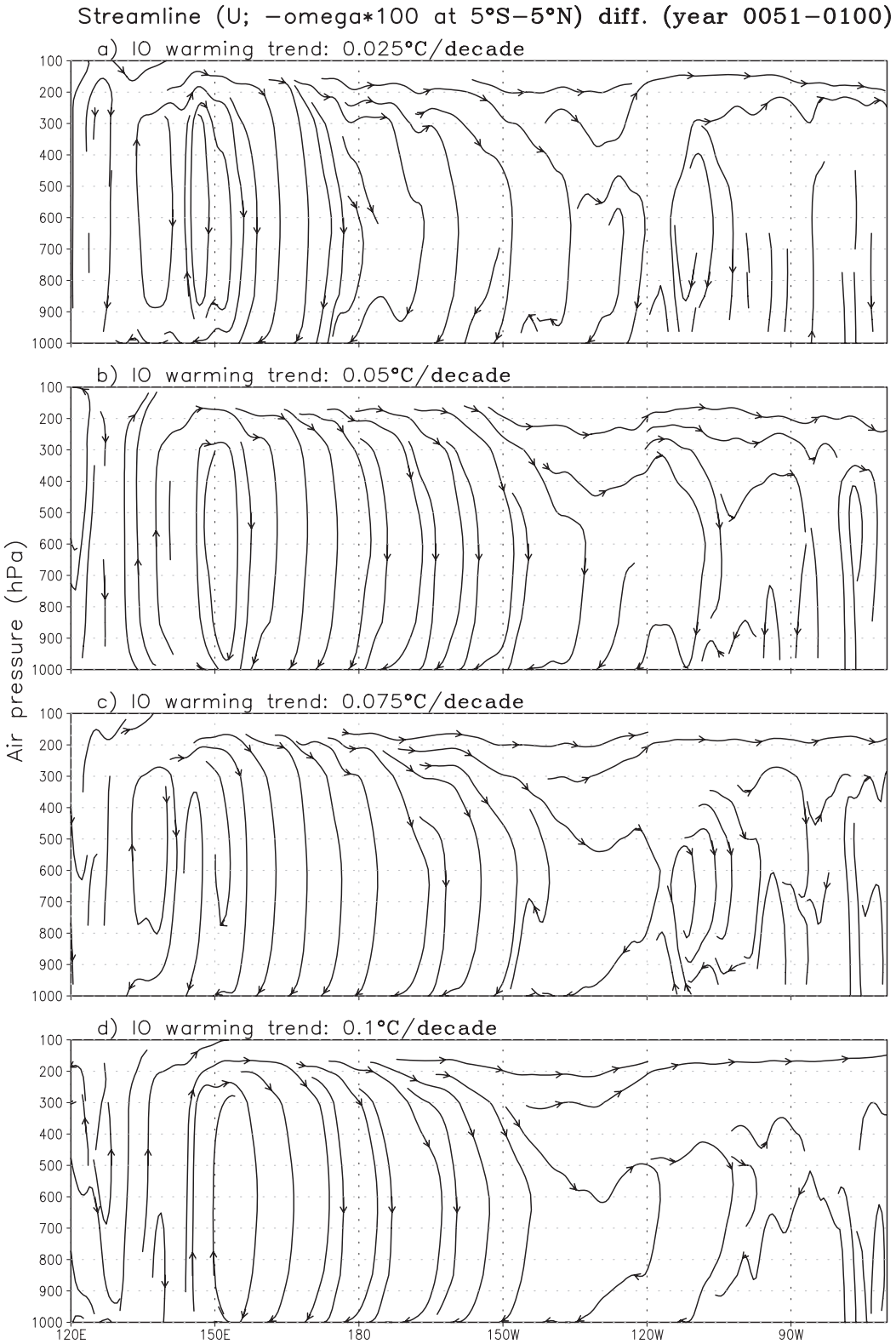

Fig. S6. Influence of the multidecadal IO warming on the Pacific Walker circulation. As in Fig. S5, but for the east–west Walker circulation change in the equatorial Pacific (5°S–5°N) due to stronger tropical IO warming (relative to the Pacific's).

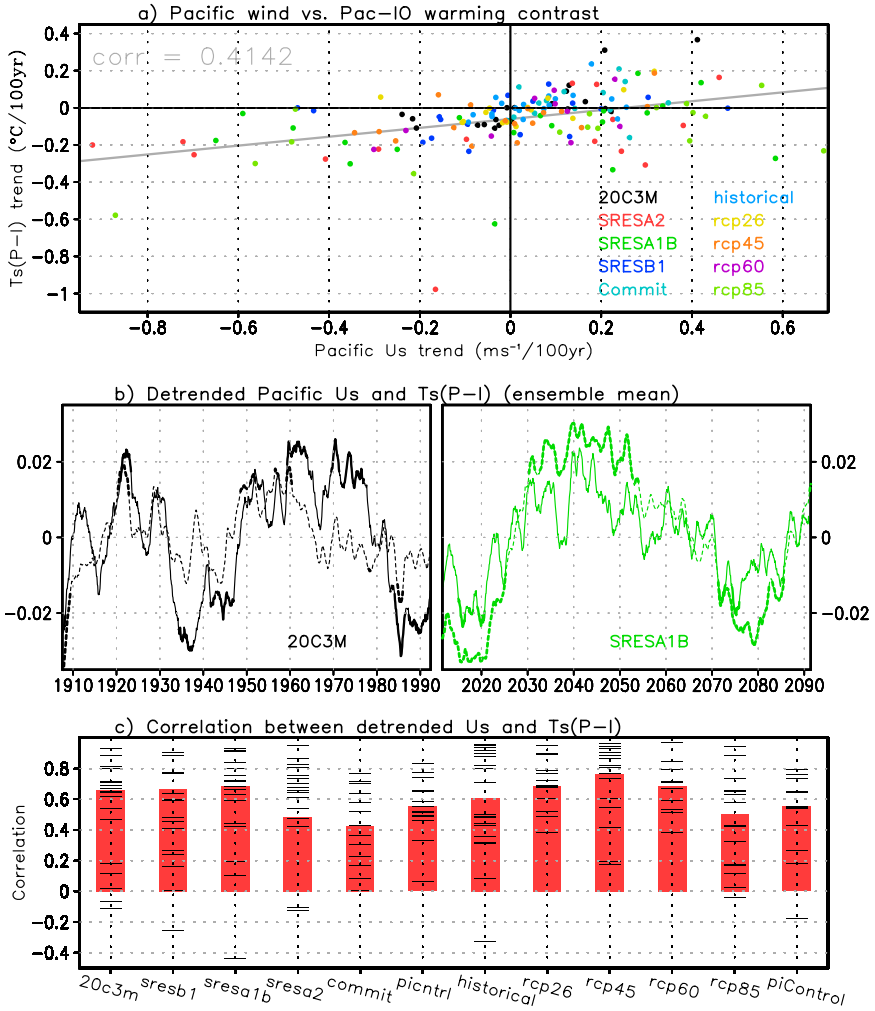

Fig. S7. Pacific wind changes modulated by the IO warming in the simulations of the "phase-3 and phase-5 of the Coupled Model Intercomparison Project" (CMIP3 and CMIP5) models. As in Fig. 4, but for the results based on the Pacific zonal winds and the SST difference between the tropical Pacific (120°–280°E, 20° S–20°N) and IO.

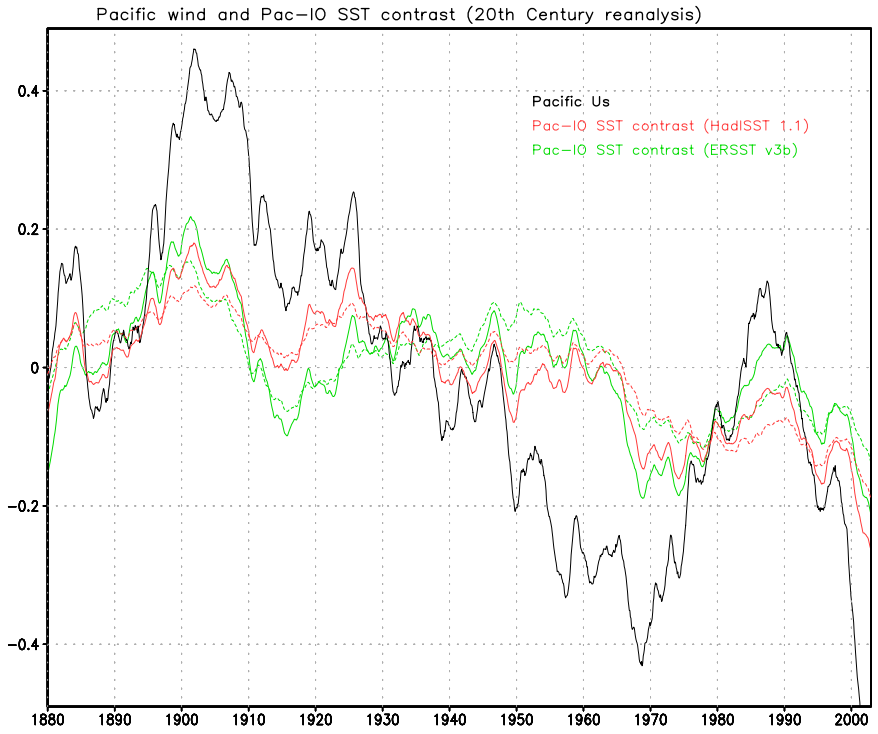

Fig. S8. Observed Pacific wind and Pacific-minus-IO SST difference in the 20th century. Shown are 15-y running mean anomalies (relative to the 1900–1999 climatology) of SST difference between the tropical eastern Pacific and IO (red solid line), SST difference between the tropical Pacific and IO (red dashed line), and Pacific zonal wind (black line) from the 20th century atmospheric reanalysis (www.esrl.noaa.gov/psd/data/gridded/data.20thC_ReanV2.html). The SST forcing is from Hadley Centre Sea Ice and Sea Surface Temperature data set (HadISST) 1.1 (badc.nerc.ac.uk/data/hadisst/). Results based on Extended Reconstructed Sea Surface Temperature (ERSST) v3b analysis are also shown (green lines). We note that data quality before early 1980s might be low owing to sparse in situ measurements (icoads.noaa.gov/r2.5.html).

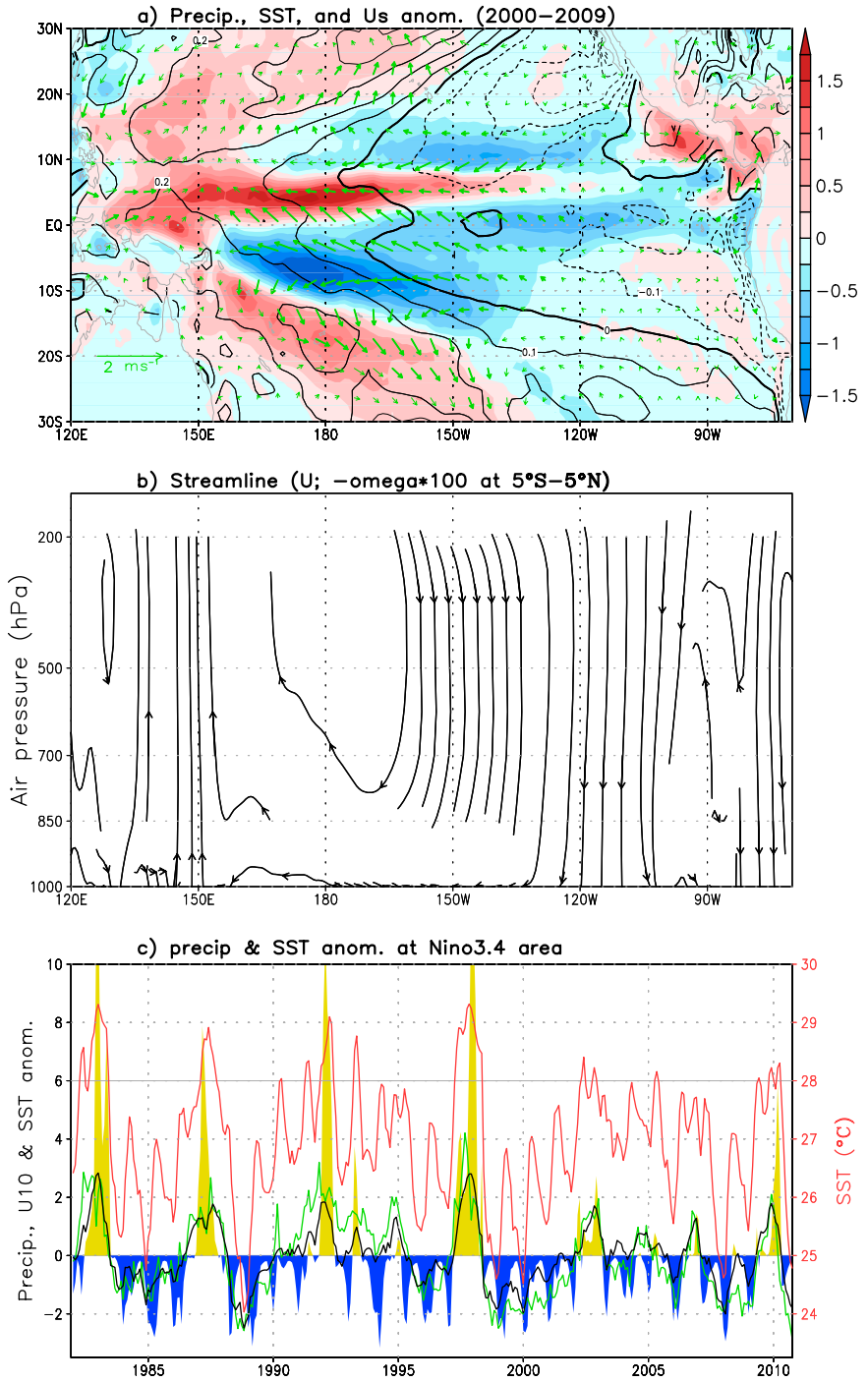

Fig. S9. Recent Pacific decadal anomalies reproduced by the climate model. Shown are 2000–2009 mean anomalies reproduced by the SINTEX-F climate model of (*A*) SST (contour), surface winds (thick vectors denote ≤5% significance according to one-tailed Student *t* test), and precipitation (mm/d, color scaled) in the tropical Pacific, and (*B*) the atmospheric Walker circulation in the equatorial Pacific. (*C*) Precipitation anomalies (line with color fill), SST anomalies (black line), and total SST (red line) at Niño3.4 area (190°–240°E, 5°S–5°N). Green line displays surface zonal wind anomalies in the central Pacific (160°–190°E, 5°S–5°N). These are based on nine-member ensemble mean of coupled model simulations with global observed SST being assimilated into the model.

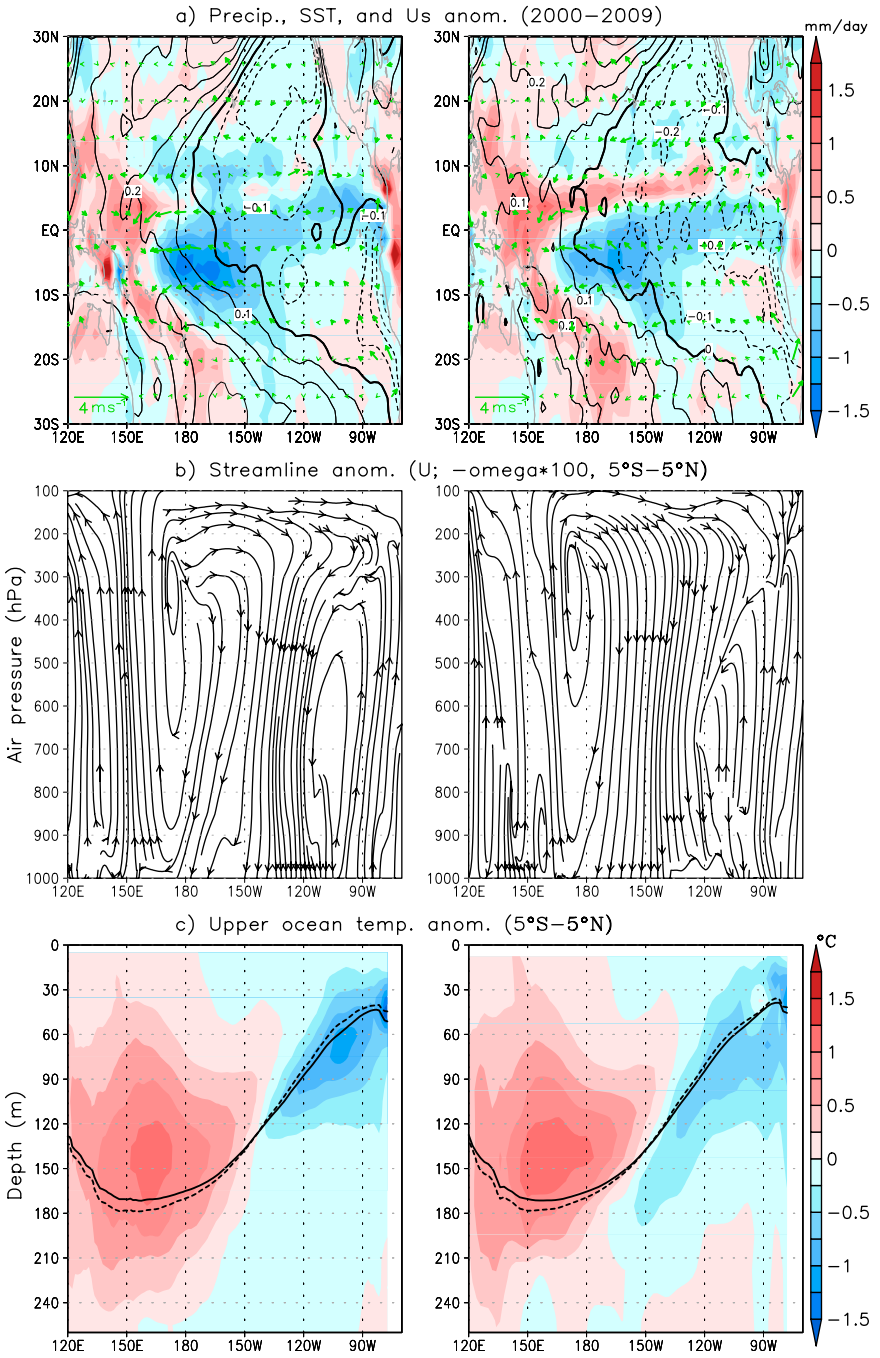

Fig. S10. Observed Pacific decadal anomalies during 2000–2009 based on other atmosphere and ocean datasets. As in Fig. 2, but for the results from (*Left*) NCEP atmosphere reanalysis (www.esrl.noaa.gov/psd/data/reanalysis/reanalysis.shtml), CPC Merged Analysis of Precipitation (CMAP) precipitation (www.cpc.ncep.noaa.gov/products/global_precip/html/wpage.cmap.html), ERSST v3b SST, and ECMWF ORA-S3 ocean analysis (www.ecmwf.int/research/EU_projects/ENSEMBLES/data/oras3_disclaimer.html); (*Right*) NCEP2 atmosphere reanalysis (www.cpc.ncep.noaa.gov/products/wesley/reanalysis2/), Global Precipitation Climatology Project (GPCP) precipitation (www.esrl.noaa.gov/psd/data/gridded/data.gpcp.html), HadISST 1.1 SST, and The Predictive Ocean Atmosphere model for Australia (POAMA) Ensemble Ocean Data Assimilation (PEODAS) ocean analysis (opendap.bom.gov.au:8080/thredds/catalog/poama/peodas/reanalysis/catalog.html).

Table S1. World Climate Research Programme CMIP3 models for each scenario experiment adopted in this analysis

Model	20C3M	SRESB1	SRESA1B	SRESA2	Commit	picntrl
BCCR BCM2.0	Y	Y	Y	Y	Y	
CCCMA_CGCM3.1 T47	Y	Y	Y	Y		Y
CCCMA_CGCM3.1 T63	Y	Y	Y			Y
CNRM CM3	Y	Y	Y	Y	Y	Y
CSIRO Mk3_5	Y	Y	Y	Y	Y	Y
GFDL CM2.0	Y	Y	Y	Y	Y	Y
GFDL CM2.1	Y	Y	Y	Y	Y	Y
GISS AOM	Y	Y	Y			
GISS-EH	Y		Y			Y
GISS-ER	Y	Y	Y	Y	Y	Y
IAP FGOALS	Y	Y	Y		Y	Y
INM CM3.0	Y	Y	Y	Y	Y	Y
IPSL CM4	Y	Y	Y	Y	Y	Y
MIROC Hires	Y	Y	Y			
MIROC Medres	Y	Y	Y	Y	Y	Y
MIUB ECHO-G	Y	Y	Y	Y	Y	Y
MPI ECHAM5	Y	Y	Y	Y		
MRI CGCM2.3a	Y	Y	Y	Y	Y	Y
U.K.MO HadCM3	Y	Y	Y	Y	Y	Y
U.K.MO HadGem1	Y		Y	Y		
Total	20	18	20	15	13	15

Detailed information on each model and experiment is available on https://esg.llnl.gov:8443/.

Table S2. World Climate Research Programme CMIP5 models for each scenario experiment adopted in this analysis

Model	Historical	RCP45	RCP60	RCP85	RCP26	piControl
BCC-CSM1-1	Y	Y	Y	Y	Y	Y
CANESM2	Y	Y		Y	Y	Y
CNRM-CM5	Y	Y		Y	Y	Y
CSIRO-MK3-6-0	Y	Y	Y	Y	Y	
GFDL-ESM2G	Y	Y			Y	Y
GFDL-ESM2M	Y					Y
GISS-E2-H	Y					Y
GISS-E2-R	Y	Y	Y	Y		Y
HADCM3	Y					
HADGEM2-CC	Y	Y		Y		
HADGEM2-ES	Y	Y	Y	Y	Y	Y
INMCM4	Y	Y		Y		Y
IPSL-CM5A-LR	Y	Y	Y	Y	Y	Y
IPSL-CM5A-MR	Y	Y		Y	Y	
MIROC-ESM	Y	Y	Y	Y	Y	Y
MIROC-ESM-CHEM	Y	Y	Y	Y	Y	
MIROC5	Y	Y	Y	Y	Y	Y
MPI-ESM-LR	Y	Y		Y	Y	Y
MRI-CGCM3	Y	Y	Y	Y	Y	Y
NORESM1-M	Y	Y	Y	Y	Y	Y
Total	20	17	10	16	14	15

Detailed information on each model and experiment is available on http://pcmdi3.llnl.gov/esgcet/home.htm/.